Available online at www.eccomasproceedia.org
Eccomas Proceedia COMPDYN (2025) 5081-509

ECCOMAS
Proceedia

COMPDYN 2025
10th ECCOMAS Thematic Conference on
Computational Methods in Structural Dynamics and Earthquake Engineering
M. Papadrakakis, M. Fragiadakis (eds.)
Rhodes Island, Greece, 15-18 June 2025

PARAMETRIC SEISMIC ANALYSIS OF HYBRID MASONRY-REINFORCED CONCRETE BUILDINGS

S. Chirivì[1], G. Blasi[1], F. Micelli[1] and M. A. Aiello[1]

[1]Department of Engineering for Innovation
University of Salento
Piazza Tancredi 7, Lecce
{salvatore.chirivi, gianni.blasi, francesco.micelli, antonietta.aiello}@unisalento.it

Abstract

Past earthquakes evidenced the high vulnerability of existing masonry buildings, mainly due to lack of ductility and, consequently, seismic energy dissipation capacity. Hence, the need of improving their seismic performance led to the adoption of different types of retrofit interventions. The insertion of internal reinforced concrete frames in existing masonry buildings was widely adopted in the last century, mainly due to architectural and functionality matters. Despite increasing the global ductility of the structural system in most of the cases, such intervention significantly modifies the response to lateral loads, alongside their distribution among the vertical elements. Hence, specific approaches should be adopted for the assessment of the seismic vulnerability of this type of hybrid masonry-reinforced concrete structures. This issue is not comprehensively addressed in modern seismic design codes, leading to the adoption of oversimplified methods for analysis and design. In this paper, the seismic response of an archetype three-storey hybrid masonry-reinforced concrete building is assessed, by performing Pushover analysis. Particularly, parametric analyses were performed to investigate the influence of the relative lateral strength and stiffness between masonry walls and reinforced concrete frame. Lastly, the effect of the seismic loads distribution among the elements on failure modes was examined depending on the relative masonry-to-frame strength and stiffness.

Keywords: Hybrid masonry-RC buildings, Seismic Performance, Pushover Analysis, Parametric Analysis.

ISSN:2623-3347
Peer-review under responsibility of the organizing committee of COMPDYN 2025.
doi: 10.7712/120125.12796.25451

1. INTRODUCTION

Since the beginning of the 20th century, the advancement of knowledge on reinforced concrete (RC) encouraged its adoption for retrofitting of existing masonry structures. Consequently, hybrid masonry-RC (HMRC) buildings became widespread, particularly in European, Mediterranean and Southern American countries [1,2]. These types of systems were rarely designed for seismic loads, mainly because of the absence of seismic design codes at the time they were constructed. Furthermore, lack of specific provision for HMRC buildings still exist in modern design codes, leading to oversimplified design assumptions [3]. Indeed, recent codes [4–10] provide only brief suggestions on structural idealization and seismic-safety oriented design criteria. Particularly, specific aspects, such as the seismic load distribution between masonry and RC elements and the influence of the type of masonry-frame connection on the global behavior, require further investigation [11].

HMRC systems are often the result of interventions on existing masonry buildings due to architectural or serviceability needs. Hence, different configurations can be observed, such as perimetral masonry walls with internal RC frames or RC walls, additional RC framed systems on top of or beside existing masonry structures [12]. A first classification of HMRC systems can be obtained by discerning "original" to "derived" hybrid masonry-RC buildings [3]. Liberatore et al. [13] proposed two macro-categories characterized by non-adherent and adherent masonry-to-RC systems, respectively, depending on their mutual interaction. Correia et al. [3] classified such buildings based on whether RC frames are added, included or substitute original masonry elements. These interventions feature increasing intrusiveness and a decreasing reversibility with respect to the original configuration.

Despite the spread of these systems, few studies investigated their complex seismic response, particularly because of hardships in laboratory testing, which require complex specimens and test setups. Tomaževič et al. [14] performed a shake table test of a three-story building with masonry perimeter walls with an internal RC frame. Negligible influence of the internal RC frame on the global performance was detected, because of the significantly lower lateral stiffness compared to the masonry elements. Jurukovski et al. [15] conducted shake table tests on 1/3-scale specimens featuring different types of hybrid structures, including a structure with perimeter masonry walls and an internal RC frame only at the first floor. The tests showed that the inclusion of RC frames or walls as strengthening intervention for masonry structures may severely affect stiffness regularity, leading to higher modes' effects. Liberatore et al. [16] performed nonlinear static analyses on a simplified structural model composed of a masonry wall connected in parallel to a RC frame. The results show the high influence of the stiffness of the connection between the two systems on the global performance. Cattari and Lagomarsino [12] evidenced the effects of the stiffness, the strength and the location of RC framed systems inserted in existing masonry buildings, on the global seismic response.

In the present study, an archetype case-study HMRC building was idealized to investigate the parameters affecting its seismic response. In particular, the building consists of masonry perimeter walls and internal RC frames. The system was modelled in STKO [17], employing non-linear models for both masonry and RC frames, to accurately estimate the response to lateral loads. Both the cases of gravity load designed and seismically designed RC elements were considered. The mutual influence of the RC frame and the masonry walls on the global seismic performance was examined through Push Over analysis, varying the relative RC frame-to-masonry stiffness. The obtained results also allowed evaluating the relationship between relative RC frame-to-masonry stiffness and failure mode of both systems.

2. ARCHETYPE HYBRID MASONRY-RC BUILDING ANALYSIS

2.1 Description of the case-study archetype HMRC building

A three-storey hybrid structure consisting of two external masonry walls rigidly connected to an internal RC frame was considered in this study (Figure 1). This HMRC structure is representative of existing masonry configurations in which the internal masonry walls were replaced by RC frames. The structural system was conceived in order to analyze the seismic response along the in-plane direction of the walls (Y-direction), neglecting the response in the out-of-plane direction, characterized by low stiffness contribution of masonry walls.

As shown in Figure 1, the structure is composed of three bays in X-direction and one bay in Y-direction, with inter-storey height and bay length equal to 3.00 m and 4.50 m, respectively. The masonry walls have dimensions of 4.50x3.00 m^2 (width x height).

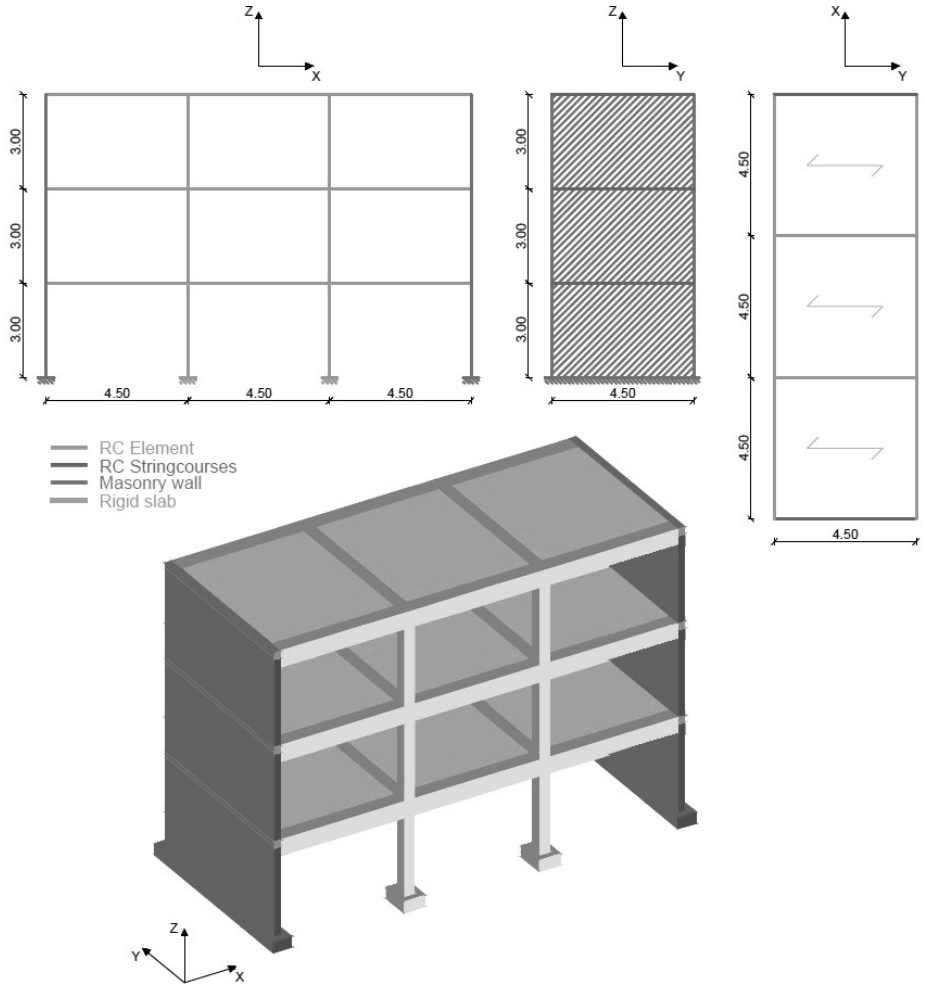

Figure 1: HMRC structure analyzed.

The mechanical properties of materials in RC frames were assumed based on usual configuration of RC framed buildings in Mediterranean regions. Particularly, the compressive strength of concrete, f_c, and yielding strength of steel rebars, f_{ys}, were equal to 25 MPa and 450 MPa, respectively. The assumption on f_c is consistent with the hypothesis of existing masonry building where internal walls were replaced with lateral load resisting RC frames. The masonry walls are composed of clay units with compressive strength equal to 9.50 MPa, according to experimental results by Morandi et al [18].

Aiming to consider the variability of the RC frames' ductility, three different configurations of the archetype building were assumed, namely a gravity loads designed system and two seismically designed systems, referred to two different seismic hazard zones in Italy, respectively. Regarding gravity load designed structure, the cross-sectional area of columns and beams was computed based on the tributary area of the slab, assuming dead and live loads equal to 7.46 kN/m^2 and to 2.0 kN/m^2, respectively. The longitudinal reinforcement was defined according to Italian building design code [8]. Seismically designed structures were designed according to an equivalent static approach [8]. A behavior factor equal to 5.85 was employed for design. The design spectrum assumed was referred to a soil type A in the areas of Benevento and Lecce, and a nominal life of the building equal to 50 years, resulting in a return period (RP) of 475 years at life safety performance level.

2.2 Description of the modelling approach

The case study HMRC structure was modelled in STKO [17]. A macro-modelling approach was adopted for masonry walls, composed of diagonal and vertical trusses to simulate the response to lateral and vertical loads, respectively. The adopted equivalent model is similar to the deformable frame model (DFM) proposed by Decret et al. [19] (Figure 2).

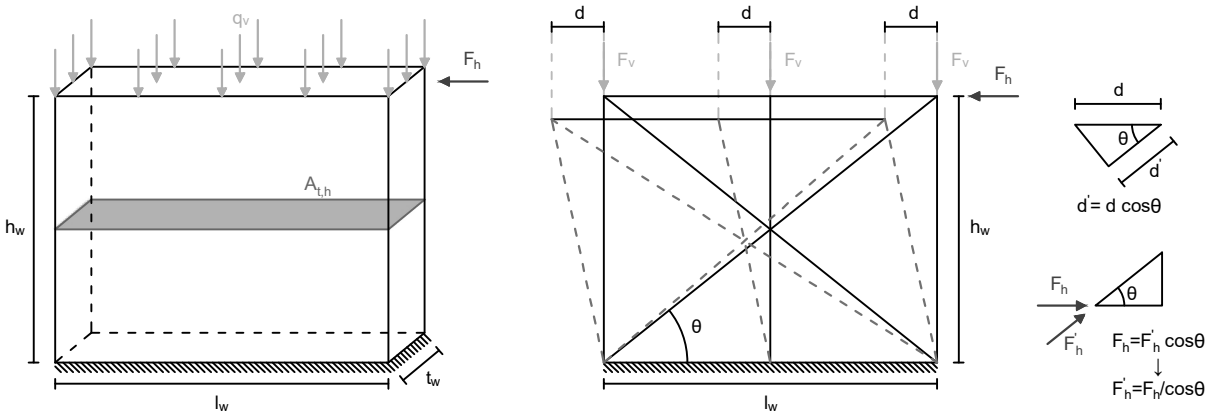

Figure 2: Truss-equivalent system proposed for masonry wall modelling.

A multilinear force-deformation (F-δ) relationship was assigned to each truss element to describe its non-linear behavior (Figure 3). In Figure 3, $F_{m,i}$, $F_{cr,i}$ and $F_{r,i}$ are the maximum, cracking and residual strength, respectively, while $\delta_{m,i}$, $\delta_{cr,i}$ and $\delta_{r,i}$ are the corresponding deformations. For better understanding of the following, the elastic stiffness, $k_{el,i}$, is also evidenced in Figure 3.

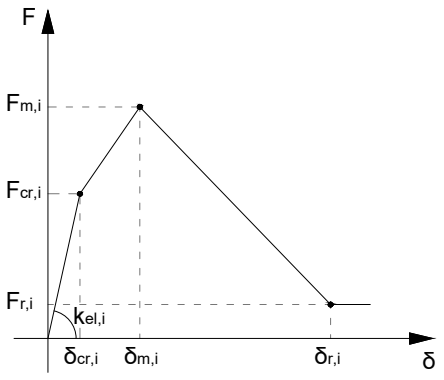

Figure 3: F-δ multilinear relationship assigned to each truss element.

The elastic axial stiffness of vertical truss element, k_v, was computed according to Equation (1):

$$k_v = \frac{E_w A_{t,h}}{3\ h_w} = \frac{E_w l_w t_w}{3\ h_w} \tag{1}$$

where l_w, h_w, t_w, E_w and $A_{t,h}$ are the width, the height, the thickness, the Young's modulus and the horizontal cross-sectional area of masonry wall, respectively.

The elastic stiffness of the diagonal truss element, k_d, is obtained as the sum in series of the flexural and the shear stiffness, k_f and k_t respectively (Equation 2):

$$k_d = k_w \frac{1}{cos^2\theta}$$
$$k_w = \frac{k_f k_t}{k_f + k_t} \qquad k_f = \frac{3\ E_w I_w}{h_w^3} = \frac{3\ E_w\ t_w \frac{l_w^3}{12}}{h_w^3} \qquad k_t = \frac{G_w A_{t,h}}{h_w} = \frac{G_w l_w t_w}{h_w} \tag{2}$$

where k_w, G_w, v_w, I_w are the lateral stiffness, the shear modulus, the Poisson's ratio and the moment of inertia of the cross section of the masonry wall, respectively, and θ is the angle of the diagonal truss with respect to the horizontal axis.

The maximum compressive strength of the vertical truss, $F_{m,cv}$, was computed according to Equation (3):

$$F_{m,cv} = \frac{F_{n,w}}{3} = \frac{f_{cv} A_{t,h}}{3} \tag{3}$$

where $F_{n,w}$ and f_{cv} are the peak axial strength and the unit vertical compressive strength of masonry. The maximum tensile strength, $F_{m,tv}$, is obtained based on the tensile strength of the mortar, assumed equal to 1/10 of its compressive strength (Equation 4):

$$F_{m,tv} = \frac{\frac{f_{cv,mo}}{10} A_{t,h}}{3} \tag{4}$$

In Equation (4), $f_{cv,mo}$ is the vertical compressive strength of mortar. The maximum axial strength of the diagonal trusses, $F_{m,d}$, was obtained based on the peak lateral strength of the wall, according to Equation (5):

$$F_{m,d} = \frac{F_w}{cos\theta} = \frac{f_{s,m} A_{t,h}}{cos\theta} = \frac{f_{s,m} l_w t_w}{cos\theta} \tag{5}$$

where F_w and $f_{s,m}$ are the peak lateral strength and the shear strength per unit area of masonry.

The cracking strength in vertical and diagonal truss elements, $F_{cr,v}$ and $F_{cr,d}$, respectively, were computed through Equation (6):

$$F_{cr,v} = F_{m,cv}\ \alpha_{cr}$$
$$F_{cr,d} = F_{m,d}\ \alpha_{cr} \tag{6}$$

where α_{cr} is a coefficient calibrated based on experimental results obtained by [18] (α_{cr} = 0.60). Residual strengths were assumed to be 30% of the maximum strengths for each truss element.

The displacements at the cracking strength of vertical and diagonal trusses, $d_{cr,v}$ and $d_{cr,d}$ respectively, and the corresponding deformations $\delta_{cr,v}$ and $\delta_{cr,d}$, were evaluated using Equation (7):

$$d_{cr,v} = \frac{F_{cr,v}}{k_v} \qquad \delta_{cr,v} = \frac{d_{cr,v}}{h_w}$$
$$d_{cr,d} = \frac{F_{cr,d}}{k_d} \qquad \delta_{cr,d} = \frac{d_{cr,d}}{h_w/sen\theta} \tag{7}$$

Lastly, the deformations corresponding to the peak and residual strength were assumed equal to $2.50 \cdot \delta_{cr,i}$ and $17 \cdot \delta_{cr,i}$, respectively, where subscript i refers to either vertical or diagonal trusses, respectively. Also these values were calibrated based on experimental results obtained by [18].

A smeared plasticity approach was used to simulate non-linear flexural response of RC beams and columns (Figure 4). Particularly, fiber-based nonlinear beam elements at the ends of the columns and of the Y-oriented beams were employed, whose length was computed according to [8]. Concrete02 and Hysteretic uniaxial materials were used for concrete and steel, respectively, in fiber-sections. X-oriented beams were modelled as linear elastic elements, as damage was not expected to occur because of the load direction considered in the analysis. Lumped shear springs were also included at the end of the columns, to simulate possible brittle shear failure. Shear springs had bi-linear rigid-softening behavior, with peak shear strength V_n, evaluated according to the variable strut inclination model [8]. The softening slope was equal to $K_{soft} = -0.8 \cdot K_{shear} = -0.8 \cdot G_c \cdot A_c / h_c$ where G_c, A_c and h_c are the shear modulus of the concrete, the cross-sectional area and the height of the column.

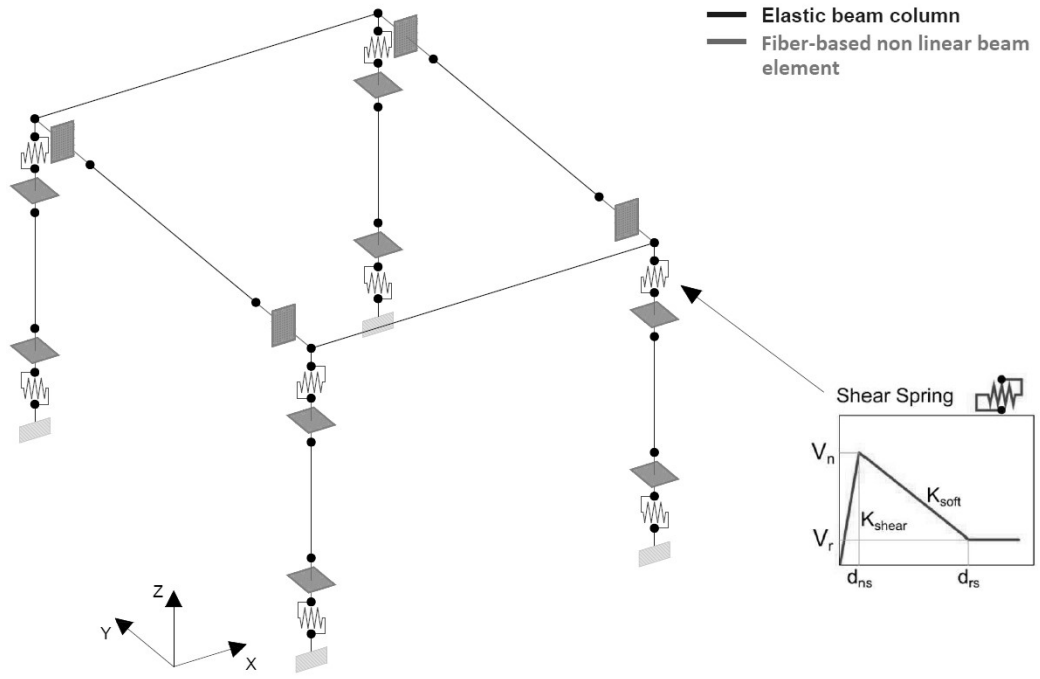

Figure 4: FE model used for the RC frame.

The slab was assumed to behave as a rigid diaphragm, and its effect was considered by including constraints at the top nodes of the columns and of the trusses simulating the masonry walls. Lastly, soil-structure interaction was neglected assuming fixed restraints at base nodes.

2.3 Parametric Analysis

The seismic performances of the considered archetype buildings were examined by conducting Push-Over (PO) analyses. The effect of the variability of relative masonry-to-RC lateral stiffness and strength on the global response and failure modes was investigated by including two coefficients α and β. Specifically, such parameters represent the masonry-to-RC frame strength ratio and the masonry-to-RC frame lateral stiffness ratio, respectively (Equation 8):

$$\alpha = \frac{F_w}{F_f}$$
$$\beta = \frac{k_w}{k_f} \tag{8}$$

In Equation (8), F_f and k_f are the lateral strength and stiffness of the RC frame, respectively.

Ten different values of β were considered for each structure, to vary masonry stiffness between 15% and 85% of the total lateral stiffness. Such boundaries were defined according to Italian building design code [8], which assumes a lateral load resisting system (LLRS) in a building as "primary system" if its lateral stiffness is at least 15% of the total lateral stiffness.

It is worth mentioning that a direct proportionality between the elastic modulus and the shear strength of masonry was considered.

An initial value of k_w was firstly defined based on a thickness equal to 200 mm, an equivalent elastic modulus equal to 2684.95 MPa and a shear strength equal to 1.07 MPa. The considered values are consistent with the data on existing databases on masonry walls [20,21]. The lateral stiffness of the so-defined masonry system was equal to 85% of the total stiffness in this case. Subsequently, the ten configurations for each considered structure (i-th structure) were defined by modifying the lateral F-δ response associated to the equivalent trusses simulating the masonry walls through the parameters α and β, according to Equation (9):

$$F_{m,i} = \alpha_i \cdot F_{f,i}$$
$$k_{el,i} = \beta_i \cdot k_{f,i} \tag{9}$$

where $F_{m,i}$ and $k_{el,i}$ are the maximum strength and the elastic stiffness of the truss elements, and $F_{f,i}$ and $k_{f,i}$ are the peak lateral strength and the elastic lateral stiffness of RC frame, for all the considered configurations.

The details of the case study HMRC structures considered are provided in Table 1 and Table 2. An ID is associated to each hybrid structure, where the symbols from left to right refer to the design type (G = Gravity loads, S = Seismic design), the site (B = Benevento, L = Lecce) and the percentage of RC frame stiffness with respect to the total stiffness, k_f%.

ID	F_w [kN]	F_f [kN]	k_w [N/mm]	k_f [N/mm]	α	β
SB_15	1926.00	236.80	395060.08	69911.70	8.13	5.65
SB_23	1728.00	236.80	236568.81	69911.70	7.30	3.38
SB_31	1530.00	236.80	158686.06	69911.70	6.46	2.27
SB_38	1332.00	315.74	112363.24	69911.70	4.22	1.61
SB_46	1134.00	315.74	81645.42	69911.70	3.59	1.17
SB_54	936.00	315.74	59788.82	69911.70	2.96	0.86
SB_62	738.00	515.49	73918.70	119266.27	1.43	0.62
SB_69	540.00	515.49	52377.11	119266.27	1.05	0.44
SB_77	342.00	515.49	35141.70	119266.27	0.66	0.29
SB_85	144.00	515.49	21037.80	119266.27	0.28	0.18

Table 1: Values of the main parameters obtained for each SB configuration.

ID	F_w [kN]	F_f [kN]	k_w [N/mm]	k_f [N/mm]	α	β
G-SL_15	1926.00	236.80	214647.06	37736.59	8.13	5.69
G-SL_23	1728.00	236.80	128273.41	37736.59	7.30	3.40
G-SL_31	1530.00	236.80	85911.31	37736.59	6.46	2.28
G-SL_38	1332.00	236.80	60768.24	37736.59	5.62	1.61
G-SL_46	1134.00	236.80	44125.36	37736.59	4.79	1.17
G-SL_54	936.00	236.80	32297.45	37736.59	3.95	0.86
G-SL_62	738.00	236.80	23484.54	37736.59	3.12	0.62
G-SL_69	540.00	236.80	16615.57	37736.59	2.28	0.44
G-SL_77	342.00	236.80	11135.08	37736.59	1.44	0.30
G-SL_85	144.00	236.80	6660.64	37736.59	0.61	0.18

Table 2: Values of the main parameters obtained for each G and SL configuration.

The cross-sectional area and the reinforcement details of columns and beams for each case are provided in Table 3 and Table 4. A constant cross-section of the columns was assumed along the height of the buildings.

ID	Cross-section		Longitudinal Reinforcement		Transverse Reinforcement	
	Base (mm)	Height (mm)	Number	Diameter (mm)	Diameter (mm)	Spacing (mm)
SB_15 SB_23 SB_31	350	350	8	14	8	160 (mid-span) 80 (ends)
SB_38 SB_46 SB_54	350	350	12	16	8	190 (mid-span) 90 (ends)
SB_62 SB_69 SB_77 SB_85	400	400	16	18	8	210 (mid-span) 100 (ends)
SL_15-85	300	300	12	14	8	160 (mid-span) 80 (ends)
G_15-85	300	300	4	12	8	140

Table 3: Cross-section dimensions and reinforcement details of columns for each case study HMRC building.

ID	Cross-section		Longitudinal Reinforcement		Transverse Reinforcement	
	Base (mm)	Height (mm)	Number	Diameter (mm)	Diameter (mm)	Spacing (mm)
SB_15 SB_23 SB_31	300	450	3+3	14	8	200 (mid-span) 80 (ends)
SB_38 SB_46 SB_54	300	450	4+4	14	8	200 (mid-span) 80 (ends)
SB_62 SB_69 SB_77 SB_85	300	450	5+5	16	8	200 (mid-span) 90 (ends)
SL_15-85	300	450	3+3	14	8	200 (mid-span) 80 (ends)
G_15-85	300	450	3+3	14	8	200

Table 4: Cross-section dimensions and reinforcement details of beams for each case study HMRC building.

3. NON-LINEAR STATIC ANALYSIS OF THE ARCHETYPE HYBRID MASONRY-RC BUILDING

For each considered configuration of the archetype building, PO analyses were performed by applying a displacement-controlled lateral load pattern with a triangular distribution in Y-direction. Such a load pattern is consistent with the in-elevation regularity of the building, which allows assuming the seismic response being dominated by the 1st mode.

The Pushover curve obtained for SB, SL and G for all the k_f% considered are shown in Figure 5.

For lower k_f% values, the global response is mainly ruled by masonry walls, which are subjected to a high ratio of the total base shear and achieve brittle failure for low values of top displacement. For higher k_f% values, the RC frame plays a more dominant role in the overall response. In these cases, the structure exhibits greater global ductility, with a significantly lower drop in post-peak load-bearing capacity. Furthermore, the displacement capacity decreases by 85%, 59% and 44% from k_f% = 85% to k_f% = 15%, for SB, SL and G, respectively.

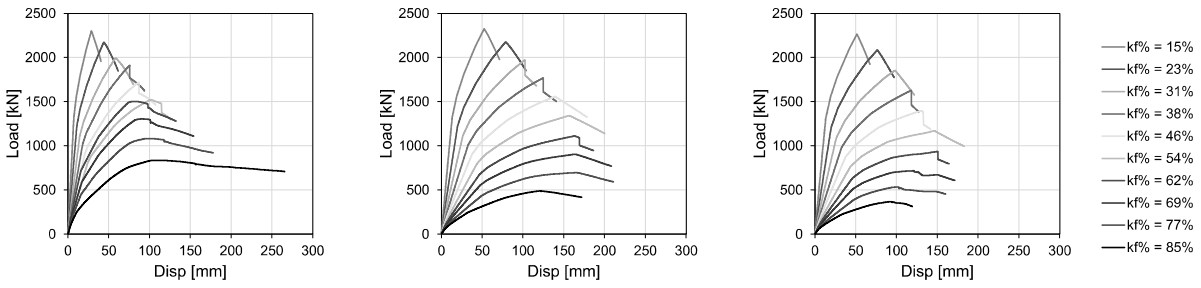

(a) (b) (c)

Figure 5: Capacity curves obtained for (a) SB, (b) SL and (c) G.

Figure 6, Figure 7 and Figure 8 show the global capacity curve (black line) alongside those referred to each structural sub-systems (red line for masonry and grey line for RC frame) for SB, SL and G, respectively. Additionally, the displacements corresponding to each detected

failure mode were evidenced. Particularly, vertical lines in figures represent the first cracking and the collapse limit state of the masonry (dashed yellow line and solid yellow line, respectively), the steel yielding limit state of RC columns (dashed purple line) and the collapse limit state of RC columns due to concrete crushing (solid green line). It is worth noting that failure mechanisms develop in a different order depending on the $k_f\%$ value.

In the case of SB (Figure 6), the first mechanism features cracking of the masonry walls, which occurs at increasingly greater displacements as $k_f\%$ rises. As expected, first cracking displacement ranges from 10 mm in the case of $k_f\%$ = 15% to around 20 mm in the case of $k_f\%$ = 62%. On the other hand, lower first cracking displacements were observed for $k_f\%$ = 85%, since as $k_f\%$ increases, the strength and stiffness of the masonry decreases.

As per collapse mechanism, masonry walls failure is firstly detected, followed by RC frame flexural collapse for all the considered cases. Particularly for both masonry and RC frame, the ultimate displacement increases with $k_f\%$, except for the case $k_f\%$ = 85%, where earlier collapse of the masonry is obtained.

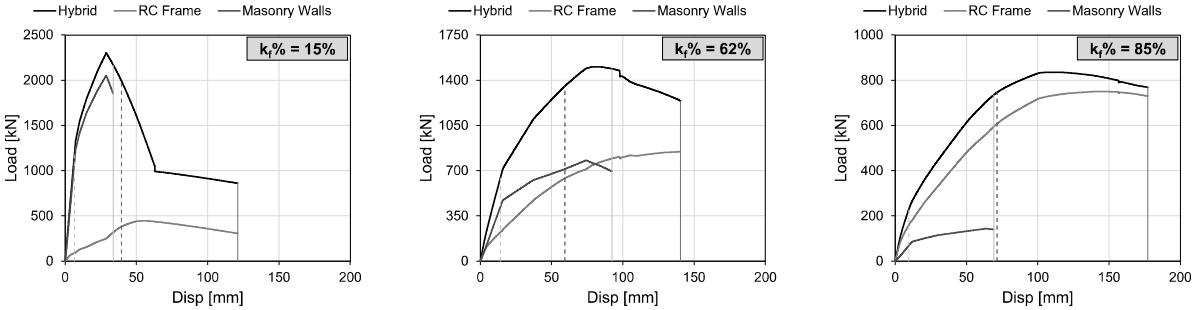

Figure 6: Capacity curves obtained for the entire HMRC building (black line) and structural sub-systems (red line for masonry and grey line for RC frame) for SB.

The same observations made for SB apply for SL (Figure 7). However, lower peak strength and elastic stiffness is obtained in SL compared to SB. Additionally, greater displacement capacity of the masonry is observed for SL compared to SB. Specifically, masonry failure in SL occurs at 60 mm, 190 mm and 150 mm for $k_f\%$ = 15%, $k_f\%$ = 62% and $k_f\%$ = 85%, respectively.

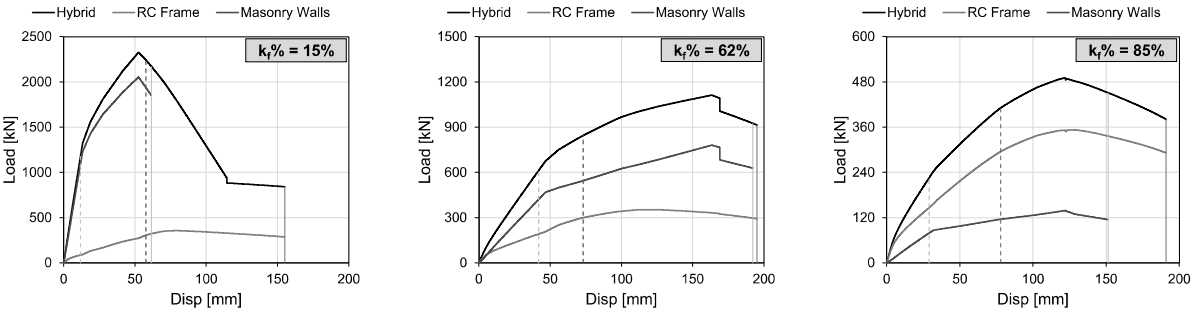

Figure 7: Capacity curves obtained for the entire HMRC building (black line) and structural sub-systems (red line for masonry and grey line for RC frame) for SL.

Lastly, Figure 8 shows the results obtained for G. Also in this case, the first mechanism is represented by masonry cracking, with a similar trend to SB. Furthermore, higher cracking displacements were observed compared to SB, namely 15 mm, 40 mm and 30 mm for $k_f\%$ = 15%, $k_f\%$ = 62% and $k_f\%$ = 85%, respectively. However, different results in terms of collapse mechanisms were obtained in this case compared to seismically designed structures. In fact, RC frame collapse precedes masonry collapse for higher values of $k_f\%$.

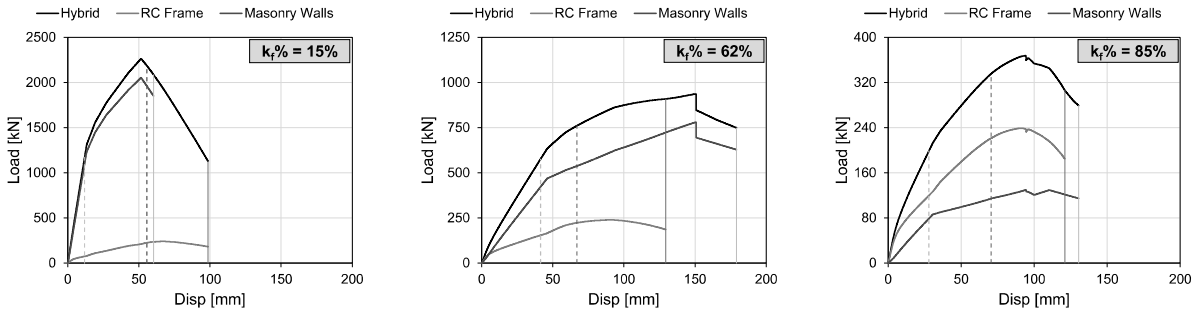

Figure 8: Capacity curves obtained for the entire HMRC building (black line) and structural sub-systems (red line for masonry and grey line for RC frame) for G.

4. CONCLUSIONS

In this study, the seismic performance of a hybrid masonry-reinforced concrete structure was examined through Push Over analysis. Different configurations of a simplified archetype structure were defined and modelled, differing from seismic detailing and relative lateral stiffness between the masonry and the reinforced concrete frame. The case-study structure is representative of existing masonry buildings, in which the internal walls were replaced by reinforced concrete frames.

The results of the Push Over analyses performed showed high influence of the relative strength and stiffness between the two systems on global displacement capacity and ductility, particularly in the case of seismically load design structures. As the lateral stiffness of the frame decreases, failure modes are increasingly affected by the masonry response, leading to brittle behavior due to early failure of the masonry walls. On the other hand, higher lateral stiffness of the reinforced concrete frames results in greater ductility and avoids early failure of the masonry.

In the case of gravity load designed frames, the contribution of masonry to lateral response is significantly higher compared to seismically design frames. Therefore, the lateral strength, the ultimate displacement capacity and the global ductility of the frame are lower compared to seismically designed frames. Hence, higher relative frame-to-wall stiffness may result in excessive seismic demand on the frame, causing early flexural collapse. This latter case is worthy of further investigation, as most of the hybrid masonry-reinforced concrete structures feature gravity load designed frames.

The analysis results showed that the accurate estimation of the optimal distribution of the global lateral stiffness among the two sub-systems is crucial when dealing with such complex buildings. The capacity curves obtained herein may lay the basis to provide code-oriented methodologies for seismic vulnerability assessment of existing hybrid structures, as well as for the design of new hybrid constructions.

REFERENCES

[1] T. Ferrito, J. Milosevic, R. Bento, Seismic vulnerability assessment of a mixed masonry–RC building aggregate by linear and nonlinear analyses. *Bulletin of Earthquake Engineering*, **14**, 2299–2327, 2016.

[2] F. Nardone, G. Verderame, A. Prota, G. Manfredi, Comparative Analysis on the Seismic Behavior of Combined RC-Masonry Buildings. *Journal of Structural Engineering*, **136**, 1483–1496, 2010.

[3] G. Correia Lopes, R. Vicente, T. Ferreira, M. Azenha, Intervened URM buildings with RC elements: typological characterisation and associated challenges. *Bulletin of Earthquake Engineering*, **17**, 4987–5019, 2019.

[4] EN 1998-1, *Eurocode 8 - Design of structures for earthquake resistance - Part 1: General rules, seismic actions and rules for buildings*, 2005.

[5] EN 1998-3, *Eurocode 8 - Design of structures for earthquake resistance - Part 3: Assessment and retrofitting of buildings*, 2005.

[6] DM-96, *D.M. 16 gennaio 1996, Norme tecniche per le costruzioni in zone sismiche*, 1996.

[7] OPCM-2005, *O.P.C.M. n. 3431/2005, Ulteriori modifiche ed integrazioni all'O.P.C.M. n. 3274/2003*, 2005.

[8] NTC-18, *Aggiornamento delle «Norme Tecniche per le Costruzioni». D.M. 17 Gennaio 2018, Italy,* 2018.

[9] Circolare 2019, *Circolare 21 Gennaio 2019 n.7 - Istruzioni per l'applicazione dell'"Aggiornamento delle «Norme tecniche per le costruzioni»" di cui al D.M. 17 Gennaio 2018, Italy,* 2019.

[10] NAA-80, *Normas Antisismicas Argentinas*, 1980.

[11] L. Liberatore, C. Tocci, R. Masiani, Non linear analyses for the evaluation of seismic behavior of mixed R.C.-Masonry structures. *Proceedings of the Seismic Engineering Conference Commemorating the 1908 Messina and Reggio Calabria Earthquake*, Reggio Calabria, Italy, July 8-11, 2008.

[12] S. Cattari, S. Lagomarsino, Seismic assessment of mixed masonry-reinforced concrete buildings by non-linear static analyses. *Earthquake and Structures*, **4**, 241–264, 2013.

[13] L. Liberatore, L. Decanini, S. Benedetti, Le strutture miste muratura-cemento armato, uno stato dell'arte. *Atti del XII Convegno Nazionale L'Ingegneria Sismica in Italia, n.90*, Pisa, Italy, June 10-14, 2007.

[14] M. Tomaževič, C. Modena, T. Velechovsky, P. Weiss, The effect of reinforcement on the seismic behaviour of masonry buildings with mixed structural system: an experimental study. *Proceedings of the ninth European Conference on Earthquake Engineering*, Moscow, Russia, 1990.

[15] D. Jurukovski, L. Krstevska, R. Alessi, P. Diotallevi, M. Merli, F. Zarri, Shaking table tests of three four-storey brick masonry models: Original and strengthened by RC core and by RC jackets. *Proceedings of 10th World Conference on Earthquake Engineering*, Madrid, Spain, July 19-24, 1992.

[16] L. Liberatore, C. Tocci, Analisi non lineari su modelli semplificati per la valutazione della risposta sismica di edifici misti muratura-c.a. *Atti del convegno Valutazione e riduzione della vulnerabilità sismica di edifici esistenti in cemento armato*, Roma, Italy, May 29-30, 2008.

[17] M. Petracca, F. Candeloro, G. Camata, STKO user manual. *ASDEA Software Technology*, Pescara, Italy, 2017.

[18] P. Morandi, G. Magenes, L. Albanesi, Prove sperimentali per la valutazione della risposta sismica nel piano di pareti murarie in blocchi di laterizio a setti sottili.

Proceedings of the XV Convegno Nazionale ANIDIS - "L'ingegneria sismica italiana," Padova, Italy, June 30-July 4, 2013.

[19] D. Decret, Y. Malecot, Y. Sieffert, F. Vieux-Champagne, L. Daudeville, A New Macro-Element for Predicting the Behavior of Masonry Structures under In-Plane Cyclic Loading. *Buildings*, **14**, 768, 2024.

[20] G. Blasi, F. De Luca, D. Perrone, A. Greco, M.A. Aiello, MID 1.1: Database for characterization of the lateral behavior of infilled frames. *Journal of Structural Engineering*, **147**, 04721007, 2021.

[21] G. Blasi, D. Perrone, M.A. Aiello, Fragility curves for reinforced concrete frames with retrofitted masonry infills. *Journal of Building Engineering*, **75**, 106951, 2023.